The EMBO Journal (2013) 32, 3206–3219
www.embojournal.org

SOURCE DATA | TRANSPARENT PROCESS

THE EMBO JOURNAL

USP10 inhibits genotoxic NF-κB activation by MCPIP1-facilitated deubiquitination of NEMO

Jixiao Niu[1,2], Yuling Shi[1,2], Jingyan Xue[2,3], Ruidong Miao[4], Shengping Huang[4], Tianyi Wang[5], Jiong Wu[3], Mingui Fu[4] and Zhao-Hui Wu[1,2,*]

[1]Department of Pathology and Laboratory Medicine, University of Tennessee Health Science Center, Memphis, TN, USA, [2]Center for Cancer Research, University of Tennessee Health Science Center, Memphis, TN, USA, [3]Department of Breast Surgery, Cancer Hospital/Institute, Fudan University, Shanghai, China, [4]Department of Basic Medical Science, University of Missouri Kansas City, Kansas City, MO, USA and [5]Department of Infectious Disease and Microbiology, University of Pittsburgh, Pittsburgh, PA, USA

DNA damage-induced activation of the transcription factor NF-κB plays an important role in the cellular response to genotoxic stress. However, uncontrolled NF-κB activation upon DNA damage may lead to deleterious consequences. Although the mechanisms mediating genotoxic NF-κB activation have been elucidated, how this signalling is terminated remains poorly understood. Here, we show that the CCCH-type zinc finger-containing protein MCPIP1 (monocyte chemotactic protein-1-induced protein-1; also known as ZC3H12A) is induced upon genotoxic treatment in an NF-κB-dependent manner. MCPIP1 upregulation reduces NEMO linear ubiquitylation, resulting in decreased activation of IKK and NF-κB. NEMO ubiquitylation is decreased through the deubiquitinase USP10, which interacts with NEMO *via* MCPIP1 upon genotoxic stress. USP10 association with NEMO leads to removal of NEMO-attached linear polyubiquitin chains and subsequent inhibition of the genotoxic NF-κB signalling cascade. Consistently, USP10 is required for MCPIP1-mediated inhibition of genotoxic NF-κB activation and promotion of apoptosis. Thus, by mediating USP10-dependent deubiquitination of NEMO, MCPIP1 induction serves as a negative feedback mechanism for attenuating genotoxic NF-κB activation.

The EMBO Journal (2013) **32,** 3206–3219. doi:10.1038/emboj.2013.247; Published online 22 November 2013
Subject Categories: signal transduction; proteins; genome stability & dynamics
Keywords: DNA damage; MCPIP1; NEMO; ubiquitylation; USP10

Introduction

An effective DNA damage response (DDR) is critical for cells to maintain genomic integrity, which is constantly challenged by genotoxic stress generated from endogeneous cell metabolism (e.g., reactive oxygen species) or environmental resources (e.g., chemicals or radiation) (Harper and Elledge, 2007; Jackson and Bartek, 2009). Failure of DDR may lead to genomic instability, which is a hallmark of cancer and ageing processes (Finkel *et al*, 2007; Hanahan and Weinberg, 2011). DDR is a comprehensive network of signalling events, which includes sensing of DNA damage, activation of cell-cycle checkpoints, recruitment of DNA repair machineries, and reprogramming of DNA damage-responsive gene expression (Jackson and Bartek, 2009; Ciccia and Elledge, 2010). Two transcription factors, tumour suppressor p53 and Nuclear Factor kappaB (NF-κB), were identified as the major transcription regulators in response to ionizing radiation (IR) (Rashi-Elkeles *et al*, 2006). While the molecular mechanisms involved in controlling p53 activity in DDR have been extensively studied, how NF-κB activation is regulated upon genotoxic stress remains poorly understood.

NF-κB is a family of transcription factors that is crucial for regulating immune responses, as well as cell survival, differentiation, and proliferation (Hayden and Ghosh, 2012). Moreover, as an inducible gene transcription regulator, NF-κB also plays pivotal roles in coordinating cellular stress responses to adapt to various mechanical, biological, and environmental stresses, including genotoxic stress. Two major signalling pathways, *classical* and *alternative* pathways, which mediate NF-κB activation following signals transduced from cytosolic membrane-bound receptors, have been well established (Perkins, 2007; Hayden and Ghosh, 2008). In addition, an atypical pathway was found to mediate NF-κB activation in response to DNA damage signals that are primarily initiated in the nucleus (McCool and Miyamoto, 2012). It was shown that IKKγ/NEMO (NF-κB essential modulator) is sumoylated in the nucleus, in a manner dependent on PIDD (p53 induced protein with death domain), PARP1 (poly(ADP-ribose) polymerase 1) and PIASy (the protein inhibitor of activated STAT), upon genotoxic stress (Huang *et al*, 2003; Janssens *et al*, 2005; Mabb *et al*, 2006; Stilmann *et al*, 2009). A DDR apical kinase, ataxia telangiectasia mutated (ATM), can then associate with and phosphorylate NEMO in the nucleus, which promotes subsequent NEMO mono-ubiquitylation and nuclear export (Wu *et al*, 2006). In the cytoplasm, NEMO can be further modified by polyubiquitin with linear linkage, which may collaborate with K63-linked polyubiquitylation of ELKS (a protein rich in glutamate, leucine, lysine, and serine) to achieve optimal activation of IKK (Wu *et al*, 2010; Niu *et al*, 2011). Additionally, ATM-dependent polyubiquitylation of TRAF6 (TNF receptor-associated factor) and/or RIP1 (receptor-interacting protein 1) may also contribute to IKK activation in response to DNA damage (Hinz *et al*, 2010; Yang *et al*, 2011).

As aberrant NF-κB activation has been linked to various pathological processes including auto-immune disorders and cancers (Ben-Neriah and Karin, 2011), negative regulation

*Corresponding author. Department of Pathology and Laboratory Medicine, Center for Cancer Research, University of Tennessee Health Science Center, 19 South Manassas Street, Memphis, TN 38163, USA
Tel.: +1 901 448 2612; Fax: +1 901 448 3910; E-mail: zwu6@uthsc.edu

Received: 23 January 2013; accepted: 31 October 2013; published online: 22 November 2013

and proper termination of NF-κB signalling are critical for maintaining cell homeostasis in response to various stresses (Ruland, 2011). Previous studies have revealed a number of mechanisms that negatively regulate NF-κB-dependent gene transcription by either inhibiting NF-κB signalling pathways in the cytoplasm or blocking chromatin binding of NF-κB in the nucleus (Ruland, 2011). Induction of several NF-κB-target genes, such as IκBα and deubiquitinase (DUB) A20, has been demonstrated to serve as critical negative feedback responses to mitigate NF-κB activation, which may control the proper magnitude and duration of NF-κB signalling. Upon DNA damage, a Sentrin/SUMO-specific protease (SENP2) was found to be induced by DNA damage in an NF-κB-dependent fashion, which inhibited NEMO sumoylation and subsequent genotoxic NF-κB activation (Lee *et al*, 2011). We showed that overexpression of CYLD, a DUB primarily disassembling K63-linked polyubiquitin in cells (Simonson *et al*, 2007), inhibited genotoxic NF-κB activation, potentially *via* inhibiting ELKS ubiquitylation upon genotoxic stimulation (Wu *et al*, 2010). However, CYLD expression was not induced by genotoxic treatment. Whether ubiquitylation can be targeted in a negative feedback manner to terminate genotoxic NF-κB activation remains elusive.

Monocyte chemotactic protein-1-induced protein-1 (MCPIP1, also known as ZC3H12A) was first identified as a potential transcription factor in cardiac myocytes regulating apoptosis and chronic inflammatory response (Zhou *et al*, 2006). Further studies indicated that MCPIP1 can be induced in macrophages to regulate inflammatory gene expression, which may involve downregulation of NF-κB signalling (Liang *et al*, 2008, 2010; Matsushita *et al*, 2009). MCPIP1-deficient mice displayed severe immune disorders as well as growth retardation and premature death (Matsushita *et al*, 2009; Liang *et al*, 2010). It was found that MCPIP1 could bind to the 3′ untranslated regions (UTRs) of a subset of inflammatory cytokine genes including *IL6* and *IL12p40*, and destabilize the bound mRNAs. A putative RNase domain was demonstrated to be essential for MCPIP1 to control the stability of those inflammatory genes (Matsushita *et al*, 2009). Intriguingly, MCPIP1 was found to negatively regulate LPS-induced NF-κB activation in macrophages by mechanisms involving removal of polyubiquitin chain from TRAF proteins, indicating that MCPIP1 may function as a DUB (Liang *et al*, 2010). Similar negative regulation of NF-κB activation by MCPIP1 was also observed in cells treated with IL-1β (Skalniak *et al*, 2009). Surprisingly, the critical domain for deubiquitinating activity of MCPIP1 was mapped to a region that also hosts the RNase activity (Liang *et al*, 2010). A recent structural study confirmed that the conformation of the putative MCPIP1 RNase domain shares high homology with the well-conserved PilT N-terminus (PIN) RNase domain (Xu *et al*, 2012). However, how MCPIP1 regulates deubiquitination remains to be delineated.

Here, we found that the transcription of MCPIP1 was upregulated, in an NF-κB dependent fashion, in cells exposed to genotoxic stimulation. Induction of MCPIP1 served as a negative feedback response to attenuate genotoxic NF-κB signalling cascade, leading to attenuation of NF-κB activation by DNA damage. MCPIP1-dependent inhibition of genotoxic NF-κB activation was mediated by USP10, which interacted with NEMO and could remove linear polyubiquitin chain attached to NEMO. Depletion of MCPIP1 or USP10 significantly increased expression of NF-κB-target genes, including inflammatory cytokines and anti-apoptotic genes, in response to genotoxic treatment. Therefore, MCPIP1 may play an important role in maintaining a balance between cell survival and inflammatory response by controlling NF-κB activation in cells exposed to DNA damage.

Results

MCPIP1 is induced by genotoxic treatments in an NF-κB-dependent manner

In our effort to identify DUBs negatively regulating genotoxic NF-κB signalling, we found that expression of MCPIP1, a protein harbouring potential deubiquitinating activity (Liang *et al*, 2010), was substantially increased in HEK293T cells in response to etoposide (Etop) treatment (Figure 1A). The increased MCPIP1 protein was commensurate to its mRNA level upon Etop treatment, suggesting that MCPIP1 induction by genotoxic treatment may be due to transcriptional upregulation (Figure 1B). Consistently, MCPIP1 expression was increased in HT1080 and MDA-MB-231 cells in response to treatment with Etop or doxorubicin (Dox), respectively (Figure 1C and D; Supplementary Figure S1A–D). It was shown that MCPIP1 transcription can be enhanced by NF-κB recruitment to its binding sites within the second intron of the *ZC3H12A* gene in cells treated with IL-1β (Skalniak *et al*, 2009). Genome-wide chromatin immunoprecipitation (ChIP)-seq data retrieved from UCSC Genome Brower also confirmed the NF-κB-binding at this transcription active regulatory region (Euskirchen *et al*, 2007) (Figure 1E, top panel). We found that inhibiting NF-κB signalling by an IKK inhibitor Bay11-7082 or overexpression of IκBα-super repressor (IκBα-SR, S32A/S36A) significantly reduced MCPIP1 induction upon DNA damage (Figure 1C and D; Supplementary Figure S1E). Moreover, we detected a significant increase in NF-κB/p65 enrichment at the NF-κB-binding sites within the second intron (enhancer region) as well as in the promoter region of *ZC3H12A* gene in response to genotoxic stimulation, which was abrogated by a more specific IKKβ inhibitor TPCA-1 (Figure 1E). Consistently, disruption of NF-κB-binding site within either promoter or enhancer of *Z3CH12A* gene abolished genotoxic drug-induced transactivation (Figure 1F), suggesting that DNA damage-activated NF-κB may directly upregulate MCPIP1 transcription. We have shown that ATM and ELKS are essential for genotoxic NF-κB signalling (Wu *et al*, 2006, 2010). Accordingly, treatment with ATM inhibitor Ku55933 substantially diminished MCPIP1 induction, as well as NF-κB enrichment at the *ZC3H12A* gene κB-binding sites, in cells exposed to genotoxic agents (Figure 1C–E). Furthermore, the upregulation of MCPIP1 transcription by DNA damage was abrogated in $ATM^{-/-}$ or $ELKS^{-/-}$ MEFs compared to wild-type (WT) cells (Figure 1G; Supplementary Figure S1F). All this body of evidence supports a critical role of NF-κB in enhancing MCPIP1 transcription upon genotoxic stress.

Induction of MCPIP1 negatively regulates DNA damage-induced NF-κB activation

MCPIP1 may regulate inflammatory gene expression by inhibiting TLR-induced NF-κB activation (Skalniak *et al*, 2009; Liang *et al*, 2010). We found that overexpression of MCPIP1 remarkably decreased Etop-induced NF-κB activation

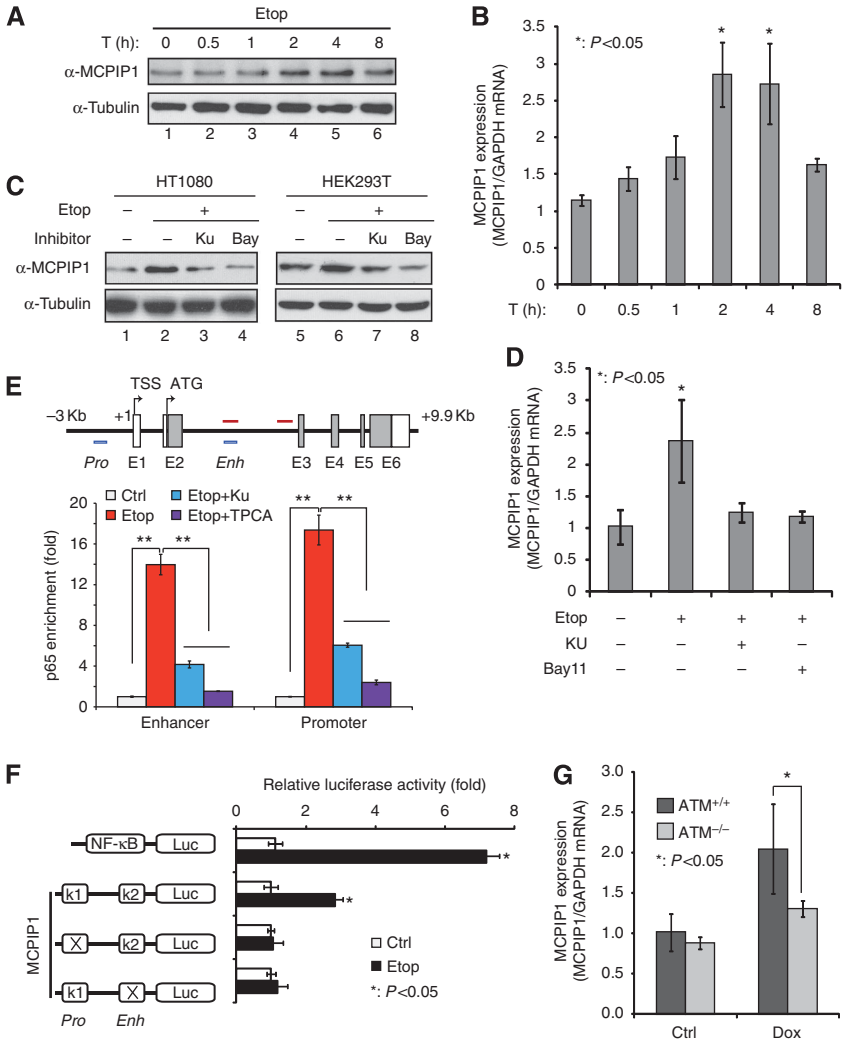

Figure 1 MCPIP1 induction by DNA damage is dependent on NF-κB. (**A**, **B**) HEK293T cells were treated with Etoposide (Etop, 10 μM) for indicated times. (**A**) Whole-cell lysates were immunoblotted with indicated antibodies. (**B**) MCPIP1 mRNA levels were measured by qRT–PCR. Relative fold induction (normalized to GAPDH) from triplicated experiments was plotted with mean ± s.d. (**C**, **D**) Indicated cells were treated with Etop (10 μM, 2 h) with or without indicated inhibitors. Immunoblotting was done as in (**A**). Ku: Ku55933 (10 μM), Bay: Bay11-7082 (10 μM). (**D**) MCPIP1 mRNA induction in HEK293T cells treated as in (**C**) was analysed by qRT-PCR as in (**B**). (**E**) Top panel: a diagram of *ZC3H12A* gene was shown. The red lines on the top indicate ChIP/Seq-identified NF-κB-binding regions retrieved from UCSC genome browser. The blue lines at the bottom indicate the region for p65 ChIP analysis in *ZC3H12A* promoter (Pro) and enhancer (Enh) regions. Bottom panel: HEK293T cells were treated as in (**D**) except for using TPCA-1 (1 μM) instead of Bay. Relative chromatin enrichment of p65 at indicated regions from triplicated experiments was plotted with mean ± s.d. $^{**}P<0.01$. (**F**) MCPIP1 promoter and enhancer region (wild type or κB-binding sites deletion mutants) as shown in (**E**) was cloned to upstream of luciferase reporter. NF-κB-reporter plasmid from Promega (pGL4.32) and MCPIP1-luciferase reporters were transfected into HEK293T cells. Normalized luciferase activity upon Etop treatments (10 μM, 6 h) from triplicated experiments were plotted as shown. X: site deletion. (**G**) $ATM^{+/+}$ and $ATM^{-/-}$ MEFs were treated with Doxorubicin (Dox, 5 μM, 2 h) or vehicle, MCPIP1 expression was measured as in (**B**). $^{*}P<0.05$.

in HT1080 cells (Figure 2A). Similarly, NF-κB activation was also inhibited by MCPIP1 in HEK293T cells exposed to IR or Etop (Figure 2B; Supplementary Figure S2). Moreover, we detected augmented NF-κB activation in $MCPIP1^{-/-}$ MEFs treated with genotoxic drugs (Figure 2C), whose duration was also extended compared to WT MEFs (Figure 2D), indicating that MCPIP1 may also negatively regulate DNA damage-induced NF-κB activation. Luciferase reporter assay further confirmed that overexpression of MCPIP1 diminished NF-κB-driven gene transactivation by genotoxic treatment (Figure 2E). Consistent with a previous report (Liang *et al*, 2010), mutation in MCPIP1 RNase domain (D141N) or Zinc finger (C306R) abolished the MCPIP1-dependent inhibition of genotoxic NF-κB activation (Figure 2A and B). However, MCPIP1 with mutation at two Asp residues (D225A/D226A), which are critical for its RNase activity (Xu *et al*, 2012), effectively inhibited genotoxic NF-κB activation (Figure 2A and B). Furthermore, reconstitution of MCPIP1-WT, but not MCPIP1-C306R mutant, substantially decreased DNA damage-induced NF-κB activation in $MCPIP1^{-/-}$ MEFs (Figure 2F). Altogether, these data indicate that NF-κB-mediated MCPIP1 upregulation may form a negative feedback response to inhibit NF-κB activation by genotoxic stress.

It was proposed that MCPIP1 may act as a DUB to inhibit NF-κB signalling by removing polyubiquitin chain from TRAFs, such as TRAF2, TRAF3, and TRAF6 (Liang *et al*, 2010). MCPIP1 has also been demonstrated to function as an RNase, which can be inactivated by mutation of Asp141 (D141N) in putative RNase domain (Matsushita *et al*, 2009). Previous studies showed that MCPIP1-D141N

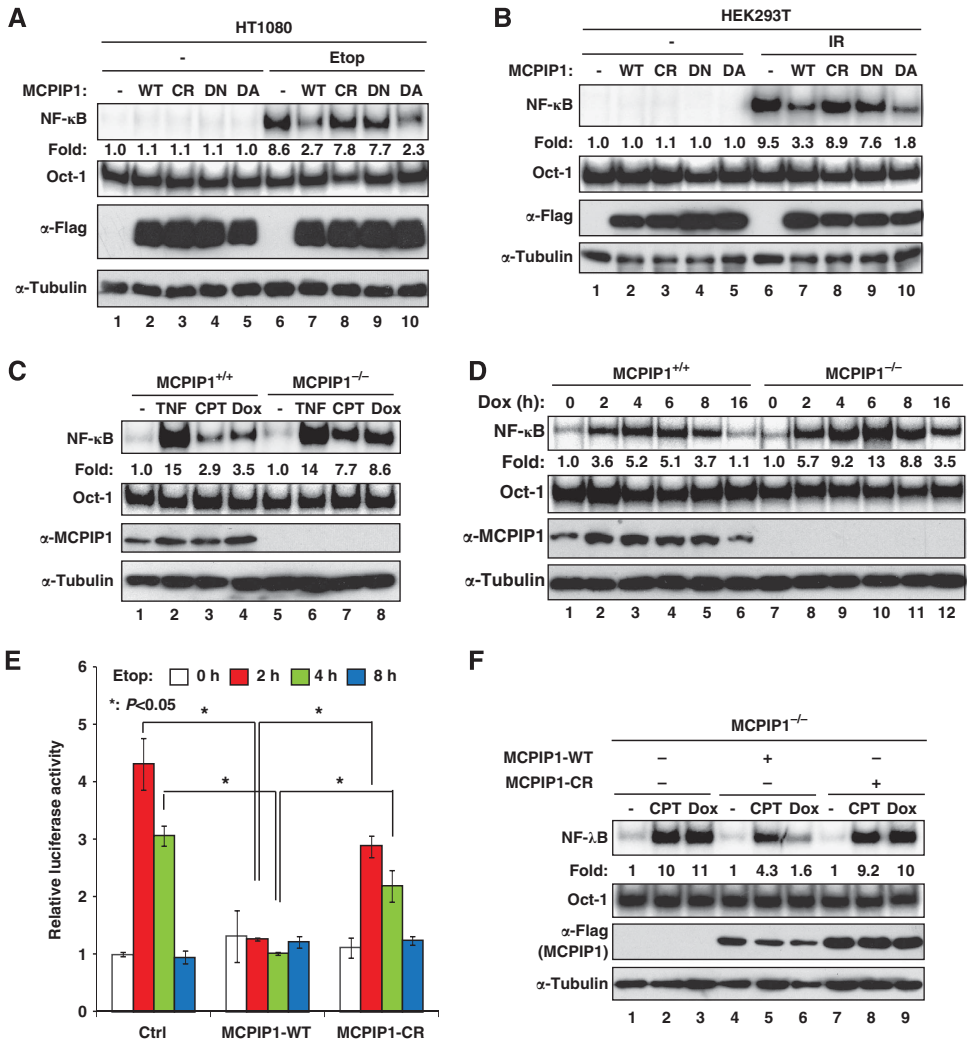

Figure 2 MCPIP1 inhibits NF-κB activation by genotoxic stress. (**A**) HT1080 cells transfected with MCPIP1-WT or mutants (MCPIP1-C306R, -D141N or -D225A/D226A) were treated with Etoposide (Etop, 10 μM, 2 h). Whole-cell lysates were analysed by EMSA and immunoblotting as shown. EMSA signals were quantified with phosphorimager and shown as fold induction. (**B**) HEK293T cell was transfected as in (**A**) and treated with IR (20 Gy). Total cell extracts were analysed at 2 h after IR as in (**A**). (**C**) MCPIP1$^{+/+}$ and MCPIP1$^{-/-}$ MEFs were treated with TNFα (10 ng/ml, 30 min), Camptothecin (CPT, 10 μM, 2 h) or Doxorubicin (Dox, 5 μM, 2 h). Whole-cell lysates were analysed by EMSA and immunoblotting as shown. EMSA signals were quantified with phosphorimager and shown as fold induction. (**D**) MCPIP1$^{+/+}$ and MCPIP1$^{-/-}$ MEFs were treated with Dox (2 μM) for times as shown, and analysed by EMSA and immunoblotting as in (**C**). (**E**) HEK293T cells transfected with κB-luciferase reporter were treated with Etop (10 μM) for times as shown. Luciferase activity form triplicated experiments was measured and relative fold induction was plotted with mean ± s.d. *$P<0.05$. (**F**) MCPIP1$^{-/-}$ MEFs were transfected with Flag-MCPIP1-WT, -C306R or vector as shown. Cells were treated and analysed as in (**C**).

mutant lost both RNase and DUB activity, whereas MCPIP1-C306R mutant only failed to cleave polyubiquitin but retained the RNase activity *in vitro* (Liang *et al*, 2010; Suzuki *et al*, 2011). We found that D141N and C306R mutation, but not RNase-inactive D225A/D226A mutation, abrogated MCPIP1-dependent inhibition of genotoxic NF-κB activation (Figure 2A and B), suggesting that the potential DUB activity may play a more important role in attenuating genotoxic NF-κB signalling than the RNase activity of MCPIP1.

MCPIP1 inhibits NEMO linear ubiquitylation and subsequent NF-κB signalling kinase activation by DNA damage

We recently showed that genotoxic NF-κB activation depended on polyubiquitylation of NEMO and ELKS with linear and K63-linked chain, respectively (Wu *et al*, 2010; Niu *et al*, 2011). Further analyses confirmed that the primary form of NEMO polyubiquitylation upon DNA damage is linear chain (Supplementary Figure S3A–C). MCPIP1 was also shown to interact with NEMO-associated IKK complex (Iwasaki *et al*, 2011). It is plausible that MCPIP1 inhibits polyubiquitylation of NEMO upon genotoxic stress, resulting in decreased NF-κB activation. Indeed, overexpression of MCPIP1 in HEK293T cells significantly reduced linear ubiquitylation of NEMO induced by genotoxic drugs (Figure 3A and B), which was not observed in cells overexpressing the MCPIP1-C306R, a mutant also failed to inhibit NF-κB activation by DNA damage (Figures 2A and 3B). Consistently, NEMO linear ubiquitylation by genotoxic treatment was diminished in cells overexpressing another MCPIP1 mutant (D225A/D226A), which also inhibited genotoxic NF-κB activation (Supplementary Figure S3D; Figure 2A and B). These data suggested that MCPIP1-mediated inhibi-

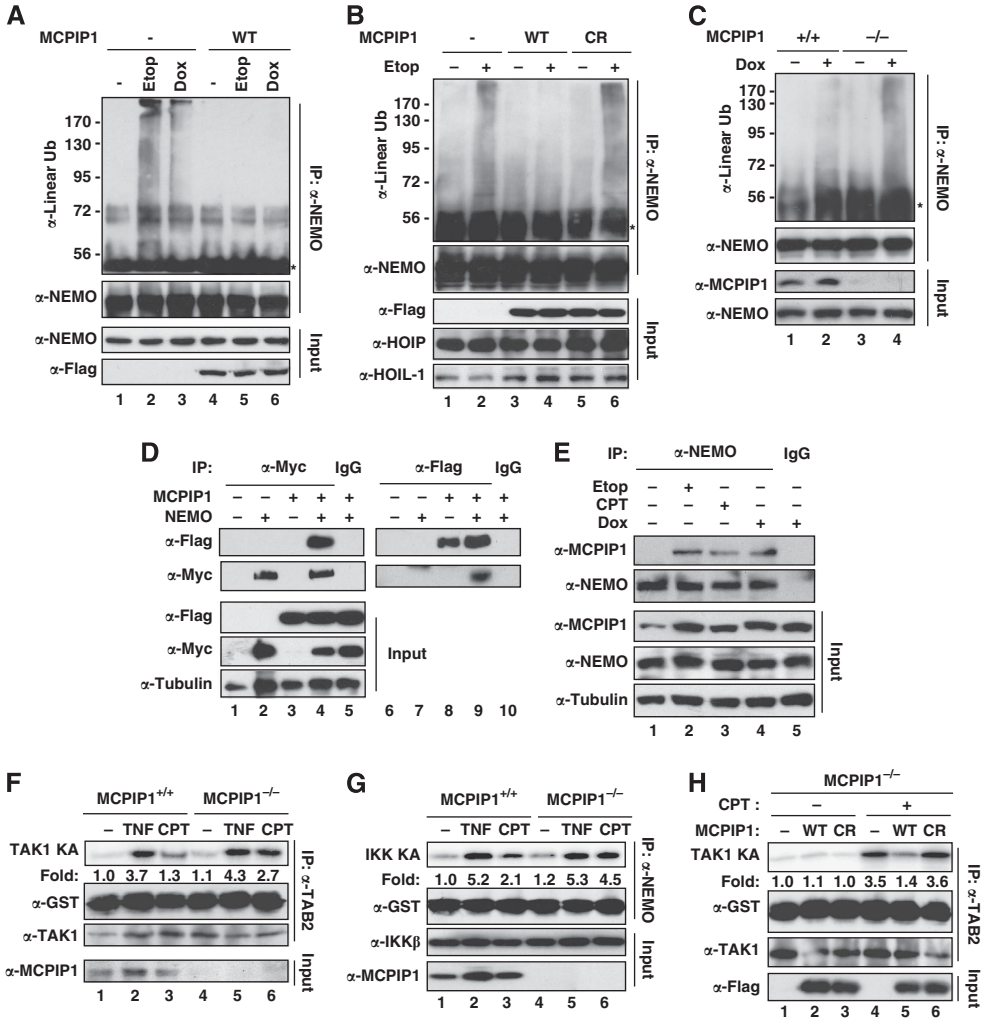

Figure 3 MCPIP1 inhibits NEMO linear ubiquitylation and subsequent kinase activation upon DNA damage. (**A**) HEK293T cells transfected with Flag-MCPIP1 or vector were treated with Etoposide (Etop, 10 μM, 2 h) or Doxorubicin (Dox, 5 μM, 2 h). Endogeneous NEMO was analysed by anti-NEMO IP followed by immunoblotting using an antibody specifically recognizing linear Ub linkage and other antibodies as indicated. *: non-specific signal. (**B**) A similar analysis as in (**A**) was performed in HEK293T cells transfected with MCPIP1-WT, -C306R or vector. (**C**) MCPIP1$^{+/+}$ and MCPIP1$^{-/-}$ MEFs were treated with Dox (5 μM, 2 h). NEMO linear ubiquitylation was analysed as in (**A**). (**D**) HEK293T cells were transfected with Flag-MCPIP1 and Myc-NEMO as indicated. Reciprocal co-IP followed by immnoblotting was performed as shown. (**E**) HEK293T cells were treated with Camptothecin (CPT, 10 μM, 2 h), Etop (10 μM, 2 h), or Dox (5 μM, 2 h) as indicated. Whole-cell lysates were IPed with anti-NEMO or IgG control and followed by immunoblotting as shown. (**F**, **G**) MCPIP1$^{+/+}$ and MCPIP1$^{-/-}$ MEFs were treated with TNF (10 ng/ml, 30 min) or CPT (10 μM, 90 min) as shown. Kinase activity of TAK1 (**F**) or IKK (**G**) was analysed by kinase assays using GST-IKKβ or GST-IκBα as a respective substrate. Substrate phosphorylation was quantified with phosphorimager and shown as fold induction. (**H**) MCPIP1$^{-/-}$ MEFs were transfected with Flag-MCPIP1-WT, -C306R or vector and treated as indicated. TAK1 kinase activity was measured as in (**F**).

tion of genotoxic NF-κB signalling correlated with its ability to antagonize NEMO linear ubiquitylation. To further delineate the impact of MCPIP1 on DNA damage-induced NF-κB signalling, we examined the NEMO ubiquitylation in Dox-treated MEFs. As expected, Dox treatment induced more prominent linear ubiquitylation of NEMO in MCPIP1$^{-/-}$ MEFs than that in MCPIP1$^{+/+}$ MEFs (Figure 3C). Our co-immunoprecipitation analyses showed that MCPIP1 associated with NEMO in HEK293 cells (Figure 3D). Furthermore, we detected an increased interaction between MCPIP1 and NEMO in response to treatment with genotoxic drugs (Figure 3E), indicating that MCPIP1 may bind to NEMO and directly promote removal of the NEMO-attached linear ubiquitin chains upon genotoxic stress.

Our previous studies demonstrated that linear ubiquitylation of NEMO is critical for DNA damage-induced sequential activation of TAK1 and IKK, which are essential for genotoxic NF-κB activation (Niu *et al*, 2011). Consistently, we found that overexpression of MCPIP1 substantially decreased activation of TAK1 and IKK by genotoxic stimulation (Supplementary Figure S3E and F). Moreover, DNA damage-induced kinase activity of TAK1 and IKK was markedly augmented in MCPIP1$^{-/-}$ MEFs, compared to the MCPIP1$^{+/+}$ cells (Figure 3F and G). Accordingly, reconstitution of MCPIP1-WT, but not the C306R mutant, attenuated the activation of TAK1 and IKK in MCPIP1$^{-/-}$ MEFs exposed to genotoxic drugs (Figure 3H; Supplementary Figure S3G). Taken together, these results further support that MCPIP1-dependent inhibition of NEMO linear ubiquitylation may diminish sequential activation of TAK1 and IKK, resulting in decreased genotoxic NF-κB activation.

MCPIP1 diminishes linear ubiquitin chain anchored on NEMO

MCPIP1 was shown to remove polyubiquitin chain attached to TRAFs, likely with K63 linkage, in splenocytes treated with LPS (Liang *et al*, 2010). It is possible that MCPIP1 may inhibit NEMO linear ubiquitylation by inhibiting K63-linked polyubiquitylation of ELKS, which was shown to promote NEMO linear ubiquitylation by DNA damage (Niu *et al*, 2011). To minimize the influence of K63-linked polyubiquitylation on linear ubiquitin chain assembly, we took advantage of an ubiquitin switching system, in which endogeneous ubiquitin can be inducibly depleted with shRNA and replaced with exogeneous ubiquitin (Xu *et al*, 2009). We confirmed that endogeneous ubiquitin was significantly decreased in cells treated with tetracycline. Simultaneously, Tet-induced expression of exogeneous ubiquitin, either WT or K63R mutant, was able to reconstitute the ubiquitin protein to the endogeneous level (Supplementary Figure S4A). However, K63-linked polyubiquitylation was abolished in K63R mutant-reconstituted cells (Supplementary Figure S4A, lane 6). We then transfected linear ubiquitylation assembly complex (LUBAC) alone, or along with MCPIP1, into these cells and examined the NF-κB activation in response to LUBAC transfection. Interestingly, although LUBAC failed to induce NF-κB activation in ubiquitin-depleted cells, we detected slightly decreased but substantial NF-κB activation in K63R ubiquitin-reconstituted cells, compared with WT ubiquitin-reconstituted cells, by LUBAC overexpression (Figure 4A, lanes 5 and 6). These data suggested that LUBAC was able to induce NF-κB activation independent of K63-linked polyubiquitin chain formation. Moreover, co-transfection of MCPIP1 significantly reduced LUBAC-induced NF-κB activation in both WT and K63R ubiquitin-reconstituted cells, suggesting that MCPIP1 could inhibit NF-κB activation by directly abrogating linear ubiquitylation of NF-κB signalling molecules such as NEMO (Figure 4A). Consistently, we found that only MCPIP1-WT, but not MCPIP1-C306R mutant, significantly inhibited LUBAC-induced NF-κB activation, confirming that the ability of inhibiting linear ubiquitylation may be essential for MCPIP1 to interrupt NF-κB activation by LUBAC (Supplementary Figure S4B).

To further delineate how MCPIP1 inhibits linear ubiquitylation, we carried out an *in vitro* DUB assay to determine the activity of immunopurified MCPIP1 to cleave polyubiquitin with linear linkage as previously reported (Liang *et al*, 2010). We found that Flag-MCPIP1 purified from HEK293T cells was able to cleave linear tetra-ubiquitin, while C306R mutation abolished this activity (Supplementary Figure S4C and D). More importantly, MCPIP1-WT, but not MCPIP1-C306R mutant, effectively removed linear polyubiquitin chains anchored on NEMO *in vitro* (Figure 4B). As we found overexpression of MCPIP1 significantly reduced DNA damage-induced NEMO linear ubiquitylation (Figure 3A and B), these data suggested that MCPIP1 may promote cleavage of linear ubiquitin chains attached to NEMO. MCPIP1 harbours an ubiquitin binding domain (UBA) at its N-terminus (Figure 4D). Deletion of this UBA domain significantly reduced the ability of MCPIP1 to inhibit genotoxic NF-κB activation (Figure 4C; Supplementary Figure S4E), which may be attributed to the decreased NEMO association and failure to inhibit NEMO linear ubiquitylation by the UBA-deletion mutant (Supplementary Figure S4F and G). Furthermore, we found that MCPIP1 directly associated with linear tetra-ubiquitin, while this association was abolished by deletion of the UBA domain (Figure 4D). MCPIP1 was shown to disassemble K63-linked polyubiquitin and its UBA domain was required for binding to ubiquitin (Liang *et al*, 2010). Our *in vitro* pull-down assay results indicated that MCPIP1-UBA could bind to both K63-linked and linear tetra-ubiquitin (Figure 4E), which may resemble the similar promiscuous specificity of the cIAP1-UBA domain reported previously (Komander *et al*, 2009).

MCPIP1-associated USP10 is essential for negative regulation of NF-κB activation

The critical region of MCPIP1 for its deubiquitylating activity was mapped to a domain that also hosts the RNase activity (Liang *et al*, 2010). A recent study revealed that the protein structure of MCPIP1 N-terminal domain shares high structural homology with the PIN domain (Xu *et al*, 2012), which is a highly conserved RNase domain. Besides, we failed to observe DUB activity of recombinant MCPIP1 protein in our *in vitro* DUB assays. These observations prompted us to consider alternative mechanisms, which may account for the DUB activity mediated by MCPIP1. In a proteomic analysis of immunopurified Flag-MCPIP1-associated protein complex by mass spectrometry, we identified a member of ubiquitin-specific protease (USP) family, USP10, as an MCPIP1-interacting protein (Supplementary Figure S5A). We further confirmed that Flag-MCPIP1 and Myc-USP10 was able to be co-immunoprecipitated reciprocally (Figure 5A). Moreover, we observed that endogeneous USP10 associated with MCPIP1, along with NEMO, in response to genotoxic stimulation, which may also be contributed by increased MCPIP1 expression (Figure 5B–D). In contrast, USP10 failed to interact with NEMO in MCPIP1$^{-/-}$ cells upon DNA damage, suggesting that MCPIP1 may serve as the scaffold for bridging USP10 association with NEMO (Figure 5C). Intriguingly, we found that MCPIP1-C306R mutant failed to interact with USP10 (Figure 5A). Furthermore, MCPIP1-D225A/226A mutant was able to associate with USP10, while D141N mutation abolished the interaction between MCPIP1 and USP10 (Figure 5E), which correlated with their ability to inhibit genotoxic NF-κB activation (Figure 2A and B). These data indicate that the interaction between MCPIP1 and USP10 is indispensable for MCPIP1-dependent inhibition of genotoxic NF-κB signalling. It is plausible that MCPIP1-mediated deubiquitination, and consequent inhibition of NF-κB signalling, is executed by an MCPIP1-associated *bona fide* DUB, such as USP10. Accordingly, MCPIP1-dependent inhibition of NF-κB activation by genotoxic drugs was abrogated by USP10 knockdown (Figure 5F; Supplementary Figure S5B). Similar results were also observed when USP10 was depleted with another siRNA targeting different sequences within USP10 (Supplementary Figure S5C). Moreover, expression of siRNA-resistant USP10 re-established MCPIP1-dependent inhibition of genotoxic NF-κB signalling in USP10-depleted cells (Figure 5F, lanes 11 and 12), indicating that USP10 is essential for MCPIP1 to attenuate NF-κB activation by DNA damage. This notion was further supported by that USP10 knockdown enhanced, while USP10 overexpression remarkably inhibited, NF-κB activation by genotoxic drugs (Figure 5G and H; Supplementary Figure S5D). Additionally, overexpression of

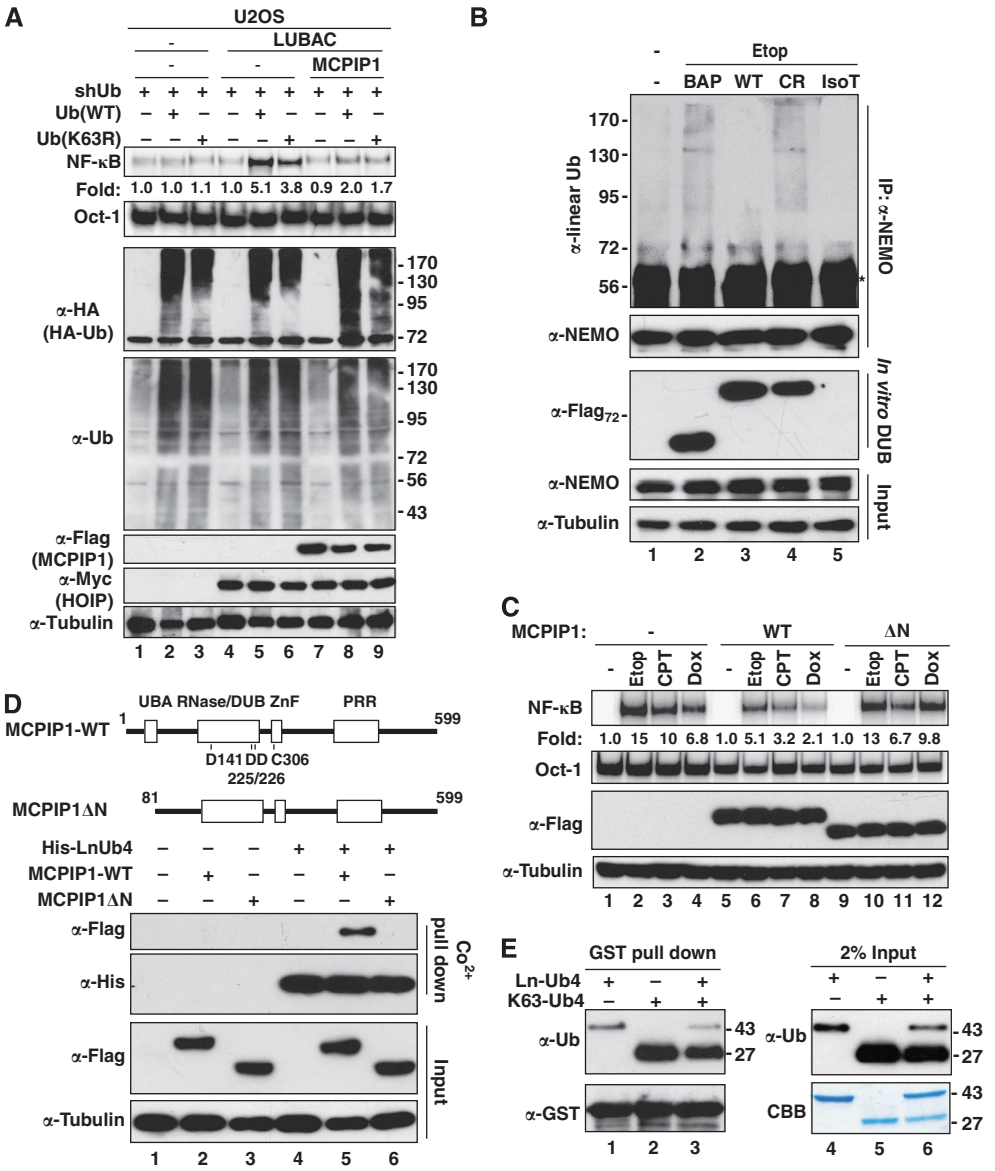

Figure 4 MCPIP1 inhibits NEMO linear ubiquitylation by DNA damage. (**A**) U2OS cells stably expressing Tet-on-shUb alone or along with Tet-Ub-WT or Tet-Ub-K63R were treated with Tetracycline (1 μg/ml). Twenty-four hours later, cells were transfected with LUBAC (HOIL-1 and Myc-HOIP) with or without Flag-MCPIP1 as indicated. Whole-cell lysates were analysed at 48 h after transfection by EMSA and immunoblotting as shown. EMSA signals were quantified with phosphorimager and shown as fold induction. HA blot was used to visualize exogeneous HA-Ub WT/K63R induced by Tet treatment. (**B**) Endogeneous NEMO was IPed from Etop-treated HEK293T cells and subjected to *in vitro* DUB assay using immunopurified Flag-MCPIP1 (WT or C306R). Purified Flag-BAP and IsoT were used as controls. NEMO linear ubiquitination was examined by immunoblotting using indicated antibodies. *: non-specific signal. (**C**) HEK293T cells were transfected with Flag-MCPIP1 WT or ΔN mutant as shown. Cells were treated with Etoposide (Etop, 10 μM, 2 h), Camptothecin (CPT, 10 μM, 2 h), or Doxorubicin (Dox, 5 μM, 2 h), and analysed by EMSA and immunoblotting as indicated. EMSA signals were quantified with phosphorimager and shown as fold induction. (**D**) Recombinant His-linear Ub_4 proteins were incubated with cell lysates from HEK293T cells expressing Flag-MCPIP1-WT or ΔN mutant. Linear Ub_4-associated proteins were analysed by immunoblotting as indicated. (**E**) Recombinant GST-MCPIP1 (UBA) was incubated with 1.5 μg of individual tetraubiquitin with K63- or linear linkage, or K63/linear tetraubiquitin mixture (1 μg:1 μg). GST-pull down complex was analysed by immunoblotting as shown. A parallel input gel was stained with GelCode blue (CBB).

USP10 in MCPIP1$^{-/-}$ MEFs barely inhibited DNA damage-induced NF-κB activation, suggesting that USP10 and MCPIP1 are mutually required for negative regulation of genotoxic NF-κB signalling (Figure 5H). In parallel, our previous studies showed that overexpression of CYLD, another USP-family DUB, attenuated genotoxic NF-κB activation by inhibiting K63-linked polyubiquitylation of ELKS, which may indirectly block NEMO linear ubiquitylation (Wu *et al*, 2010; Niu *et al*, 2011). However, knockdown of CYLD did not abolish MCPIP1-dependent inhibition of NF-κB activation and consequent gene transcription upon genotoxic stress (Supplementary Figure S5E and F). Taken together, these data strongly suggest that USP10 is a specific DUB responsible for MCPIP1-dependent inhibition of genotoxic NF-κB signalling.

USP10 removes linear ubiquitin chain attached to NEMO upon DNA damage

USP10 was identified as a DUB that could translocate into nucleus and deubiquitinate p53 in response to DNA damage (Yuan *et al*, 2010). A Cys-to-Ala mutation (C424A) at catalytic

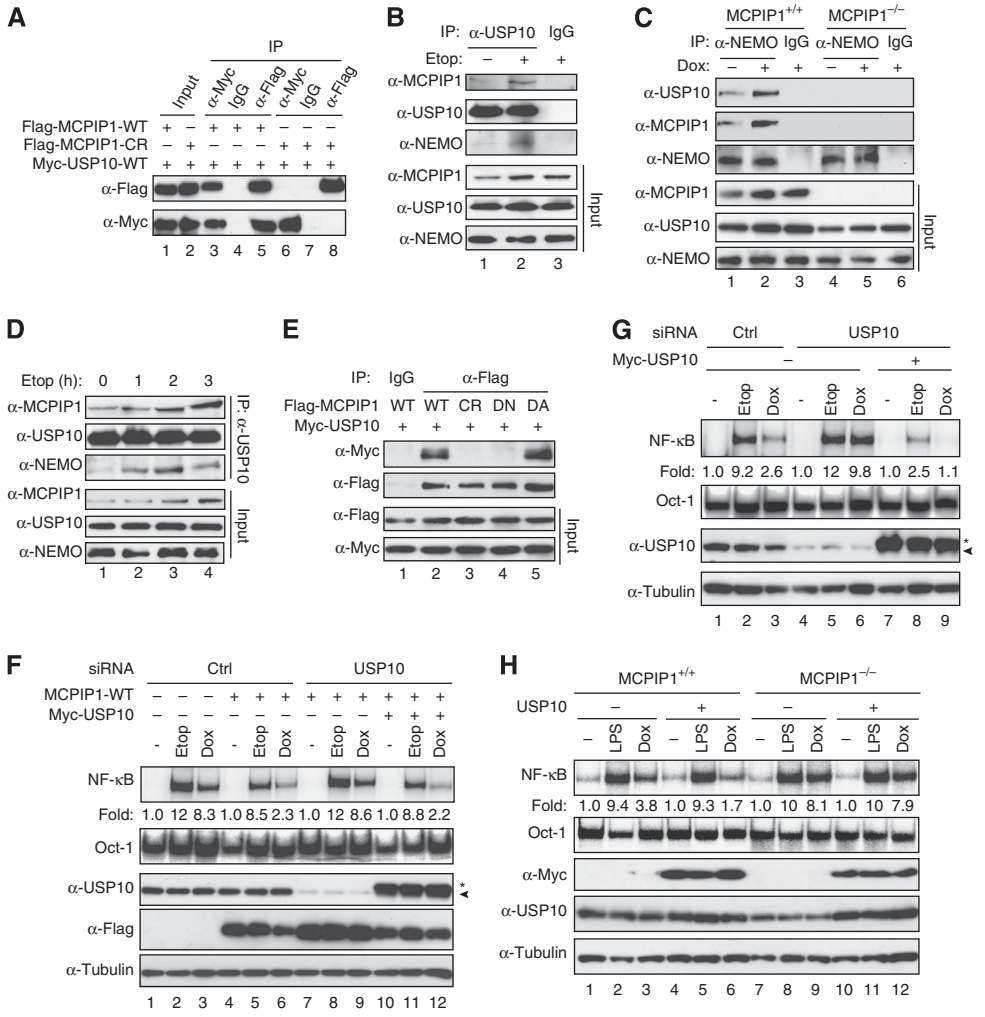

Figure 5 MCPIP1-associated USP10 is essential for inhibition of genotoxic NF-κB activation. (**A**) HEK293T cells were transfected as indicated. Whole-cell lysates were IPed with anti-Myc, anti-Flag or IgG followed by immunoblotting as shown. (**B**) HEK293T cells were treated with Etoposide (Etop, 10 μM, 2 h). Whole-cell lysates were analysed by anti-USP10 IP followed by immunoblotting using indicated antibodies. (**C**) MCPIP1$^{+/+}$ and MCPIP1$^{-/-}$ MEFs were treated with Doxorubicin (Dox, 5 μM, 2 h). Whole-cell lysates were IPed with anti-NEMO and analysed by immunoblotting as in (**B**). (**D**) HEK293T cells were treated with Etop (10 μM) for times as indicated. Whole-cell lysates were subjected to IP with anti-USP10 antibody and immunoblotted with antibodies as indicated. (**E**) HEK293T cells were transfected with MCPIP1-WT or mutants (C306R, D141N, and D225A/D226A) along with USP10 as shown. Whole-cell lysates were IPed with anti-Flag and IgG followed by immunoblotting as indicated. (**F**) HEK293T cells were transfected with control or USP10 siRNA with or without siRNA-resistant Myc-USP10. Cells were treated and analysed as shown. (**G**) HEK293T cells were transfected and treated as indicated. Whole-cell lysates were analysed by EMSA and immunoblotting as in (**F**). Arrowhead: endogeneous USP10; Star: siRNA-resistant Myc-USP10. (**H**) MCPIP1$^{+/+}$ and MCPIP1$^{-/-}$ MEFs were transfected with Myc-USP10 and treated with LPS (10 μg/ml, 30 min) or Dox (5 μM, 2 h). Whole-cell lysates were analysed by EMSA and immunoblotting as shown.

domain abrogates USP10 DUB activity (Soncini *et al*, 2001), which also abolished its ability to deubiquitinate and subsequently stabilize p53 upon DNA damage. Consistently, we found that USP10-CA mutant failed to inhibit DNA damage-induced NF-κB activation, indicating that the DUB activity is critical for USP10-dependent negative regulation of genotoxic NF-κB signalling (Figure 6A). Since we found that MCPIP1 facilitated association between USP10 and NEMO (Figure 5B and C), and MCPIP1 promoted disassembly of NEMO linear ubiquitylation (Figure 3A–C), we speculated that USP10 may inhibit NEMO linear ubiquitylation upon genotoxic stress. Indeed, overexpression of USP10, but not its catalytic inactive CA mutant, substantially reduced NEMO linear ubiquitylation in response to Etop treatment (Figure 6B). Moreover, we detected substantial increase in NEMO linear ubiquitination upon genotoxic stimulation in cells depleted of USP10 (Figure 6C). Consistently, USP10-WT, but not its C424A mutant, was able to remove linear polyubiquitin attached on NEMO *in vitro* (Figure 6D and E). Interestingly, recombinant USP10 protein purified from insect cells efficiently cleaved HA-tagged ubiquitin hexamer with linear linkage *in vitro* (Soncini *et al*, 2001). We also found that DUB domain of recombinant USP10 is sufficient for cleaving tetraubiquitin with linear linkage (Supplementary Figure S6B and C), while it cleaves K63-linked tetraubiquitin more efficiently (Supplementary Figure S6C). These results were further confirmed in assays using purified human USP10 from HEK293T cells (Supplementary Figure S6D and E). In addition, MCPIP1-dependent inhibition of NEMO linear ubiquitylation was abolished by USP10 knockdown (Figure 6F). Altogether, these data strongly support that MCPIP1-mediated inhibition

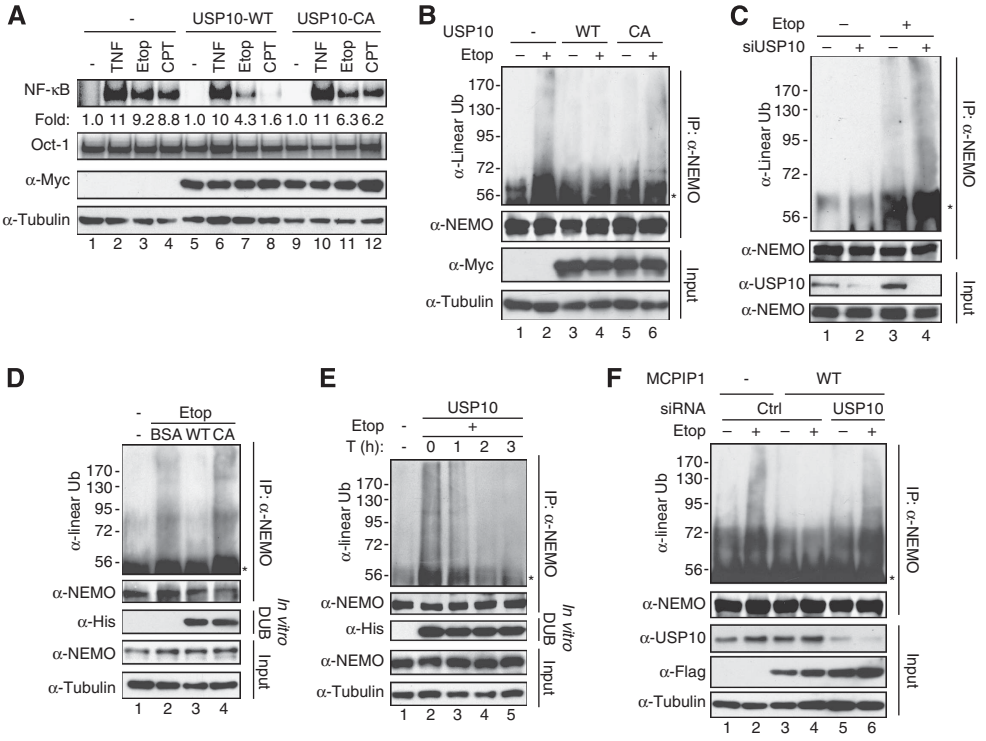

Figure 6 USP10 cleaves NEMO-anchored linear ubiquitin chains. (**A**) HEK293T cells were transfected with Myc-USP10-WT or -C424A mutant. Cells were treated with TNFα (10 ng/ml, 30 min), Camptothecin (CPT, 10 μM, 2 h), or Etoposide (Etop, 10 μM, 2 h) and analysed by EMSA and immunoblotting as shown. EMSA signals were quantified with phosphorimager and shown as fold induction. (**B**) HEK293T cell transfected as in (**A**) was treated with Etop (10 μM, 2 h). Endogeneous NEMO was analysed by anti-NEMO IP followed by immunoblotting as shown. (**C**) HEK293T cells were transfected with control siRNA or siRNA targeting USP10. Cells were treated with Etop and analysed as in (**B**). (**D**) Ubiquitylated NEMO was IPed from Etop-treated HEK293T cells and incubated with recombinant USP10 (WT or C424A) or BSA for 4 h at 37°C. The reaction was stopped by 4 × Laemmli buffer and analysed by immunoblotting using indicated antibodies. (**E**) Similar DUB assay using USP10-WT as in (**D**) was carried out for times as indicated. (**F**) HEK293T cells were transfected and treated as shown. Endogeneous NEMO was IPed and analysed as in (**B**). *: non-specific signal.

of NEMO ubiquitylation in genotoxic NF-κB signalling depends on USP10, which may cleave linear polyubiquitin chains from NEMO.

To determine whether USP10-dependent inhibition of genotoxic NF-κB signalling relies on its activity to cleave polyubiquitin with non-linear linkage, such as K63-linked chain, we depleted LUBAC-catalytic component HOIP in HEK293T cells. Interestingly, we were able to detect genotoxic drug-induced NF-κB activation at a much reduced level in HOIP-depleted cells, compared to that in WT cells. However, this reduced NF-κB activation by DNA damage was no longer sensitive to USP10 overexpression (Supplementary Figure S6F). On the other hand, we found that etoposide treatment induced substantial NF-κB activation in K63R-Ub-replaced U2OS cells, which was inhibited by overexpression of USP10-WT, but not USP10-C424A mutant (Supplementary Figure S6G). These results are in accordance to our observation that MCPIP1 was able to inhibit LUBAC-induced NF-κB activation in K63R-Ub-replaced U2OS cells (Figure 4A), suggesting that MCPIP1/USP10-mediated DUB activity against K63-chain is dispensable for MCPIP1/USP10-depedent inhibition of genotoxic NF-κB activation.

MCPIP1 regulates expression of pro-inflammatory cytokines at both transcriptional and post-transcriptional levels

MCPIP1 was shown to destabilize the mRNA of a subset of pro-inflammatory cytokines, such as IL-6 and IL-12p40, which maintains static level of these inflammatory cytokines and prevents immune disorders (Matsushita *et al*, 2009; Iwasaki *et al*, 2011). We found that, besides IL-6, mRNA levels of TNFα and Cox-2 were also substantially increased in MCPIP1$^{-/-}$ cells. Moreover, the induction of these inflammatory cytokines was further augmented in MCPIP1$^{-/-}$ cells, compared to that in MCPIP1$^{+/+}$ cells, upon genotoxic treatment (Supplementary Figure S7A). Consistently, knockdown of USP10 was able to rescue the MCPIP1-mediated repression of the inflammatory cytokine induction by DNA damage (Supplementary Figure S7B). It was shown that the mRNA stability of certain inflammatory cytokines such as TNFα and CXCL1 was not regulated by MCPIP1 (Matsushita *et al*, 2009). Therefore, the escalated induction of TNFα mRNA level in MCPIP1$^{-/-}$ MEFs upon DNA damage plausibly was due to enhanced transcription by NF-κB activation in these cells. In contrast, both increased NF-κB activation and decreased mRNA decay may contribute to the augmented IL-6 mRNA level in MCPIP1$^{-/-}$ MEFs treated with genotoxic drugs.

MCPIP1/USP10-dependent inhibition of NF-κB activation promotes apoptosis upon genotoxic stress

Our previous studies showed that DNA damage-induced NF-κB activation promotes cell survival by upregulating anti-apoptotic genes such as *BIRC2/BIRC3* and *BCL2L1* (Wu *et al*, 2010; Niu *et al*, 2011). We found that overexpression of MCPIP1 in HEK293T and HT1080 cells markedly increased

the activity of the Caspases in response to Etop treatment (Figure 7A; Supplementary Figure S8A). In contrast, MCPIP1 deficiency significantly enhanced MEF cell survival upon IR or Dox treatment (Supplementary Figure S8B and C). Consistently, upregulation of anti-apoptotic genes, including *BIRC2/BIRC3* and *BCL2L1*, was significantly increased in MCPIP1-deficient cells exposed to Dox (Figure 7B). Furthermore, Caspase 3 activation enhanced by MCPIP1 overexpression was attenuated by USP10 knockdown in cells treated with Etop (Figure 7C). In addition, USP10 depletion also reversed the repression of anti-apoptotic gene induction by overexpressing MCPIP1 in genotoxic drug-treated cells (Figure 7D; Supplementary Figure S8D). Furthermore, USP10 knockdown significantly enhanced cIAP1/2 and Bcl-xL transcription while inhibited Caspase 3 activation in Etop-treated cells (Supplementary Figure S8E and F). All these data suggest that MCPIP1/USP10-mediated inhibition of genotoxic NF-κB signalling and subsequent attenuation of anti-apoptotic gene induction may be responsible for augmented apoptosis upon DNA damage.

To validate our observation from cell culture models *in vivo*, we treated MCPIP1$^{+/+}$ and MCPIP1$^{-/-}$ mice with IR. Interestingly, intestinal tissue from MCPIP1$^{-/-}$ mice displayed substantially high basal NF-κB activation

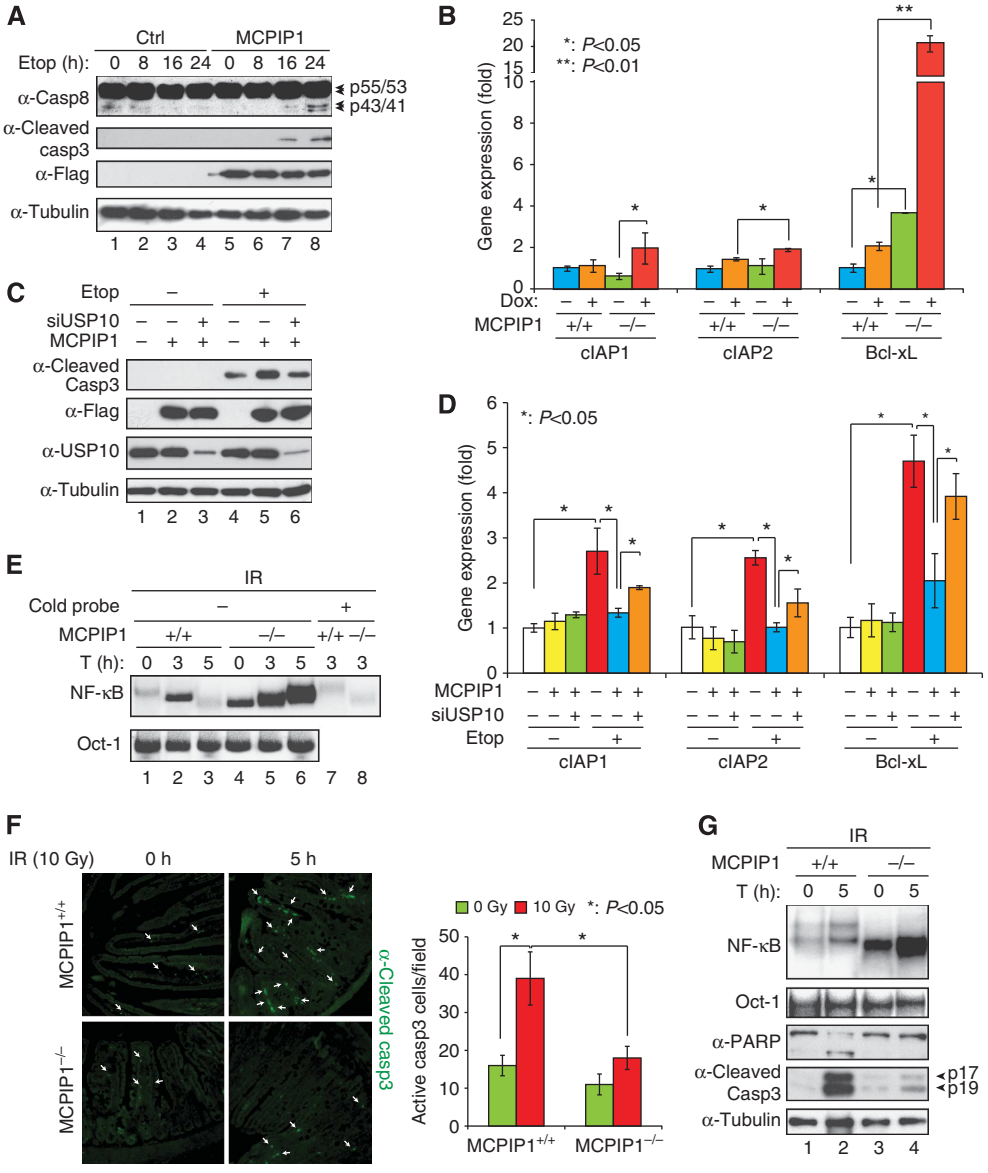

Figure 7 MCPIP1 and USP10 promote apoptosis in cells exposed to genotoxic stress. (**A**) HEK293T cells were transfected with control or MCPIP1 construct. Cells were treated with Etoposide (Etop, 10 μM) for indicated times. Whole-cell lysates were analysed by immunoblotting as shown. (**B**) MCPIP1$^{+/+}$ and MCPIP1$^{-/-}$ MEFs were treated with Doxorubicin (Dox, 5 μM, 4 h). Expression of indicated genes was determined by qRT-PCT. Relative fold-induction (normalized to GAPDH) from triplicated experiments was plotted with mean ± s.d. (**C**) HEK293T cells were transfected with MCPIP1 and siUSP10 as shown. Cells were treated with Etop (10 μM, 24 h) and analysed as in (**A**). (**D**) HEK293T cells were transfected as in (**C**) and treated with Etop (10 μM, 4 h). Indicated gene induction was analysed as in (**B**). Normalized fold induction from triplicated experiments was plotted with mean ± s.d. (**E**) Proximal intestine tissues of MCPIP1$^{+/+}$ and MCPIP1$^{-/-}$ mice were collected at indicated times after IR (10 Gy). Intestine protein extracts were analysed by EMSA with or without cold NF-κB-probe competition. (**F**) Proximal intestine tissues from MCPIP1$^{+/+}$ and MCPIP1$^{-/-}$ mice were collected in sham-treated mice or 5 h after IR (10 Gy). Active-Casp3 was visualized with immunofluorescence. Quantification of cells with active Casp3 was shown as mean ± s.d. (**G**) Intestine samples collected as in (**F**) were analysed by EMSA and blotted as indicated. *$P<0.05$; **$P<0.01$.

compared to MCPIP1$^{+/+}$ mice. Consistent with our results in genotoxic drug-treated cells, IR induced much more robust and extended NF-κB activation in small intestine of MCPIP1$^{-/-}$ mice than that in MCPIP1$^{+/+}$ mice (Figure 7E). We further confirmed that IR-induced Caspase 3 activation was significantly attenuated in intestinal tissues of MCPIP1$^{-/-}$ mice (Figure 7F and G), likely due to augmented NF-κB activation in response to IR treatment (Figure 7E). Altogether, these results further support that MCPIP1 plays a critical role in regulating apoptosis in response to radiation *in vivo*, likely *via* modulating NF-κB-dependent gene transcription.

Discussion

In this report, we found that MCPIP1 was induced in cells treated with genotoxic agents. The upregulation of MCPIP1 appeared to mainly depend on NF-κB-mediated transactivation of the *ZC3H12A* gene. A previous report showed that a transient degradation of MCPIP1 was required for its induction by LPS, as MCPIP1 may destabilize its own mRNA (Iwasaki *et al*, 2011). However, we did not observe an evident decrease in MCPIP1 protein level following genotoxic treatments (Figure 1A; Supplementary Figure S1B). This could be explained by the notion that genotoxic stress may not induce activation of IKK and IRAK1 simultaneously, whereas MCPIP1 phosphorylation by both kinases was required for its proteasome-dependent degradation (Iwasaki *et al*, 2011). Since DNA damage upregulated MCPIP1 expression without inducing its degradation, it is plausible that additional mechanisms, such as temporary inhibition of MCPIP1 RNase activity, may be involved in regulating MCPIP1 induction by DNA damage. Our data indicated that MCPIP1 induction may serve as a negative feedback response to mitigate NF-κB activation in cells exposed to genotoxic stress. Moreover, we found little evidence that MCPIP1, as a predominantly cytoplasmic protein, directly affects DNA damage signalling in response to genotoxic treatments (Supplementary Figure S9). The MCPIP1-mediated inhibition of genotoxic NF-κB signalling was dependent on USP10. USP10 can be recruited to ubiquitylated NEMO through MCPIP1 and cleaves the NEMO-attached linear polyubiquitin chains, resulting in inhibition of IKK and subsequent NF-κB activation by DNA damage. As a key signalling molecule involved in genotoxic NF-κB activation, NEMO can be modified with a series of reversible modifications, including sumoylation, phosphorylation, mono-ubiquitylation, and linear polyubiquitylation, in response to DNA damage (McCool and Miyamoto, 2012). Since NF-κB-dependent induction of SENP2 also inhibits genotoxic NF-κB signalling by diminishing NEMO sumoylation (Lee *et al*, 2011), it is plausible that all these reversible modifications of NEMO, as well as those of other proteins (e.g., ELKS, RIP, and TRAF6) involved in genotoxic NF-κB signalling, may serve as rheostats for regulating the magnitude and duration of NF-κB activation upon DNA damage (Figure 8).

The function of linear ubiquitylation in regulating NF-κB signalling is well recognized (Iwai, 2012; Rieser *et al*, 2013). While much has been learned about formation of linear ubiquitin chain, little is known how linear chains are disassembled. Two latest elegant studies identified an OTU domain-containing DUB, OTULIN (also known as Fam105B or gumby), which specifically cleaves linear ubiquitin chain and was shown to negatively regulates TNFα-induced NF-κB activation and promote Wnt signalling (Keusekotten *et al*, 2013; Rivkin *et al*, 2013). Whether OTULIN negatively regulates genotoxic NF-κB activation remains to be determined. Although NEMO is the only linear-ubiquitylated protein identified in genotoxic NF-κB signalling so far, it is possible that additional proteins participating in this signalling can also be modified with linear ubiquitin chain upon genotoxic stress. Whether USP10 and/or OTULIN can attenuate genotoxic NF-κB activation by inhibiting linear polyubiquitylation of other proteins, besides NEMO, warrants further investigation.

MCPIP1 was shown to function as both RNase and DUB. Surprisingly, the critical domains responsible for these two enzyme activities were mapped to a significantly overlapped region (Matsushita *et al*, 2009; Liang *et al*, 2010). While multiple lines of evidence supported that this region adopts a structural conformation of the PIN-RNase domain and is essential for MCPIP1 RNase activity, the mechanism by which this domain affects MCPIP1-dependent DUB

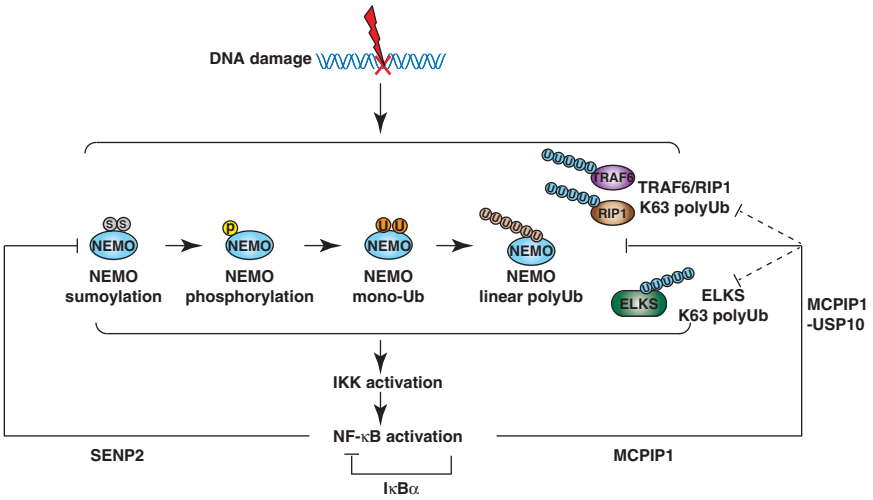

Figure 8 A model illustrates MCPIP1/USP10-mediated negative regulation of DNA damage induced NF-κB signalling.

regulation is unclear. Our data from *in vitro* DUB assay showed that immunopurified USP10 cleaved tetra-ubiquitin much more efficiently than MCPIP1, indicating that the MCPIP1-associated USP10 may be responsible for the DUB activity of the MCPIP1 immunocomplex. This was further supported by evidence that knockdown of USP10 abolished the activity of MCPIP1 to inhibit NEMO ubiquitylation and genotoxic NF-κB signalling. Moreover, mutation in MCPIP1 RNase domain (D141N) and Zn finger region (C306R) disrupted MCPIP1 association with USP10, which may explain why the RNase domain appeared to be essential for the DUB activity of MCPIP1. Therefore, two N-terminal domains of MCPIP1 are indispensable for MCPIP1 to regulate USP10-dependent deubiquitination. The RNase-CCCH domain is required for interaction between MCPIP1-NEMO-USP10 and the UBA domain is required for MCPIP1 binding to ubiquitin chains, which may present the ubiquitylated substrates to USP10 for cleavage. It is possible that additional interactions between MCPIP1 and NEMO as well as potential direct association between USP10 and polyubiquitin could further enhance the cleavage of NEMO linear ubiquitin chain by USP10 upon genotoxic stress.

USP10 primarily resides in the cytoplasm in resting cells. Upon DNA damage, USP10 is stabilized and a fraction of USP10 can translocate into the nucleus, where it deubiquitinates and stabilizes p53, leading to increased apoptosis (Yuan *et al*, 2010). USP10 also inhibits ubiquitylation of Beclin1, leading to Beclin1 stabilization (Liu *et al*, 2011). Interestingly, accumulated Beclin1 reciprocally stabilizes USP10, resulting in increased p53 and apoptosis. Here, we showed that USP10 may also participate in DDR by deubiquitinating NEMO in the cytoplasm. NEMO was found to be modified by two types of ubiquitylation, mono-ubiquitylation in the nucleus and linear polyubiquitylation in the cytoplasm, in cells exposed to genotoxic stress (Huang *et al*, 2003; Niu *et al*, 2011). Our data indicated that MCPIP1 induction upon DNA damage enhanced interaction between USP10 and NEMO. USP10 may cleave the linear polyubiquitin chains attached to NEMO, which could disrupt the ubiquitin scaffolds required for optimal IKK activation and subsequent NF-κB activation. Although cleavage of peptide bonds linking linear ubiquitin chain by USP10 may contribute to diminishing NEMO ubiquitylation, our data suggest that the removal of linear ubiquitin chains form NEMO likely to be mediated primarily by USP10-depedent cleavage of an isopeptide bond between NEMO and the first ubiquitin moiety, which remove the linear chain entirely. Nevertheless, considering the activity of USP10 in cleaving K63-linked and proteolysis-targeting polyubiquitin chains, it is possible that USP10 may also inhibit other upstream ubiquitylation events, such as ELKS ubiquitylation, which are required for optimal NEMO linear ubiquitylation and NF-κB activation in cells exposed to genotoxic stress. In addition, USP10-dependent stabilization of p53 upon DNA damage may negatively regulates NF-κB-dependent transcription by competing for limiting pools of coactivators, such as p300 and CBP (Tergaonkar and Perkins, 2007). These potential mechanisms could be involved in USP10-dependent inhibition of NF-κB activation. Therefore, USP10 may functionally coordinate the programmed cell death in response to DNA damage by enhancing p53 activity while inhibiting NF-κB activation, which may depends on its promiscuous DUB activity in cleaving diverse ubiquitin linkages.

Besides regulating apoptosis, MCPIP1 plays a critical role in controlling inflammatory response. MCPIP1-deficient mice displayed severe immune disorders and died prematurely (Matsushita *et al*, 2009; Liang *et al*, 2010). Considering the important roles of NF-κB in regulating both inflammation and apoptosis, it is plausible that MCPIP1-dependent inhibition of NF-κB may also significantly contribute to a balanced stress response between cell survival and inflammation. In response to pathogen infection or genotoxic stress, NF-κB is activated to promote cell survival as well as coordinate inflammatory response. However, uncontrolled NF-κB activation may lead to deleterious consequences such as hyper-inflammation and tumorigenesis (Ruland, 2011). DNA damage-induced NF-κB in general is believed to promote cell survival by upregulating anti-apoptotic genes. Nevertheless, excessive and prolonged DNA damage-induced NF-κB activation may substantially upregulate TNFα, which could lead to a TNFα feed-forward signalling promoting apoptosis (Biton and Ashkenazi, 2011). We found that DNA damage-induced MCPIP1, by attenuating NF-κB activation, not only inhibited anti-apoptotic gene transcription but also reduced induction of inflammatory cytokines such as IL-6 and TNFα. Therefore, MCPIP1-mediated negative feedback control of NF-κB activation may serve as a critical mechanism to mitigate damage by hyper-inflammation and prevent tumorigenesis upon genotoxic stress.

Materials and methods

Chromatin immunoprecipitation

The ChIP analyses were performed following the manufacturer's protocol (Pierce). In brief, cells were cross-linked with 1% formaldehyde, sheared to an average size of ~500 bp and followed by immunoprecipitation with a p65 antibody (C-20, Santa Cruz). Immunoprecipitated antibody/protein/DNA complexes were digested with protease K and DNA was eluted. P65 enrichment was quantified by real-time PCR using primers listed in Supplementary Table S1.

Immunoprecipitation and immunoblotting

For co-IP experiments, cells were lysed in 10% PBS and 90% Lysis buffer (20 mM Tris (pH 7.0), 250 mM NaCl, 3 mM EDTA, 3 mM EGTA, 0.5% NP-40, 2 mM DTT, 0.5 mM PMSF, 20 mM β-glycerol phosphate, 1 mM sodium orthovanadate, 1 μg/ml leupeptin, 1 μg/ml aprotinin, 10 mM *p*-nitrophenyl phosphate, 10 mM sodium fluoride). In all, 1 μg of indicated antibody or IgG control was added to lysates and incubated with protein G-Sepharose at 4°C overnight. Sepharose-enriched immunocomplexes were resolved on SDS–PAGE, transferred onto PVDF membrane and analysed with immunoblotting.

To detect ubiquitinated form of NEMO, cells were lysed with 1% SDS in IP lysis buffer, incubated at 95°C for 30 min, then diluted to 0.1% SDS with lysis buffer and subjected to immunoprecipitation with anti-NEMO antibody. The transferred nitrocellulose membrane was further boiled in water for 30 min, and then probed with antibody against linear chain-specific ubiquitin and visualized by ECL according to the manufacturer's instructions.

RNA extraction, reverse transcription and quantitative real-time PCR

Total RNA was extracted with Trizol (Invitrogen, Grand Island, NY) and retro-transcribed with Superscript III (Invitrogen). Real-time PCR analyses were performed in triplicate as previously described (Niu *et al*, 2012). The sequences of gene-specific primers used for quantitative real-time PCR (qPCR) are shown in Supplementary Table 1. The housekeeping gene GAPDH was used as an internal control, and gene expression was calculated using comparative CT method.

Ub replacement assay
Endogeneous ubiquitin depletion and replacement assay was performed as reported (Xu *et al*, 2009). Briefly, U2OS cells expressing Tet-on shUb alone or along with Tet-on-Ubwt or -UbK63R were treated with tetracycline (1 μg/ml). In all, 48 h (shUb-Ubwt/K63R cells) or 24 h (shUb cells) later, cells were transfected with constructs as indicated in figures. Cells were harvested at 48 h after transfection and total cell extracts were analysed by EMSA and immunoblotting.

In vitro deubiquitination assay
The DUB assay was performed following a previous report (Komander *et al*, 2009). Briefly, Flag-MCPIP1 or Flag-USP10 was purified from HEK293T cells transfected with respective plasmid using the Flag M purification kit (Sigma). Recombinant His-USP10 proteins were purified from *E. coli* using Cobalt beads. All purified proteins (0.5 μg) were incubated in an activation buffer (25 mM Tris (pH 7.5), 150 mM NaCl and 10 mM DTT) at room temperature for 10 min. Reaction was then performed in the diluted enzyme mixed with tetraubiquitin (K63-lined or linear, BioMol) and 10 × DUB buffer (500 mM NaCl, 500 mM Tris (pH 7.5) and 50 mM DTT) at 37°C for indicated times. Reactions were terminated by adding 4 × SDS loading buffer; and samples were examined by western blotting with ubiquitin antibody. Purified Flag-BAP (Sigma, P7582) and IsoT (BioMol) were used as a negative or positive control, respectively. For NEMO deubiquitylating assays, ubiquitylated NEMO immunoprecipitated under stringent lysis condition was used as the substrate.

Supplementary data
Supplementary data are available at *The EMBO Journal* Online (http://www.embojournal.org).

Acknowledgements

We thank Drs Zhijian Chen (UT-Southwestern) for Ub-replacement U2OS cells, Kazuhiro Iwai (Kyoto University) for linear-Ub specific antibody and expression constructs of HOIL1 and HOIP, Feng Shao (NIBS) for His-linear tetraubiquitin construct, Miklos Bekes and Tony Huang (New York University) for HA-Ub-K11 only construct, and Drs S Miyamoto, L Pfeffer and R Laribee for stimulating discussion and critical reading of the manuscript. We are grateful to Dr Jos Domen for helping with mouse IR experiments. This work was supported in part by NIH CA149251, American Cancer Society (RSG-13-186-01-CSM) and Methodist translational cancer research grant (all to Z-HW), and NIH HL098794 (MF).

Author contributions: Z-HW and JN designed the experiments, analysed the data, and wrote the manuscript. JN, YS, JX, RM, SH, TW, and Z-HW performed the experiments. All authors discussed the results and contributed to the final manuscript.

Conflict of interest

The authors declare that they have no conflict of interest.

References

Ben-Neriah Y, Karin M (2011) Inflammation meets cancer, with NF-[kappa]B as the matchmaker. *Nat Immunol* **12:** 715–723

Biton S, Ashkenazi A (2011) NEMO and RIP1 control cell fate in response to extensive DNA damage *via* TNF-[alpha] feedforward signaling. *Cell* **145:** 92–103

Ciccia A, Elledge SJ (2010) The DNA damage response: making it safe to play with knives. *Mol Cell* **40:** 179–204

Euskirchen GM, Rozowsky JS, Wei C-L, Lee WH, Zhang ZD, Hartman S, Emanuelsson O, Stolc V, Weissman S, Gerstein MB, Ruan Y, Snyder M (2007) Mapping of transcription factor binding regions in mammalian cells by ChIP: Comparison of array- and sequencing-based technologies. *Genome Res* **17:** 898–909

Finkel T, Serrano M, Blasco MA (2007) The common biology of cancer and ageing. *Nature* **448:** 767–774

Hanahan D, Weinberg RA (2011) Hallmarks of cancer: the next generation. *Cell* **144:** 646–674

Harper JW, Elledge SJ (2007) The DNA damage response: ten years after. *Mol Cell* **28:** 739–745

Hayden MS, Ghosh S (2008) Shared principles in NF-kappaB signaling. *Cell* **132:** 344–362

Hayden MS, Ghosh S (2012) NF-κB, the first quarter-century: remarkable progress and outstanding questions. *Genes Dev* **26:** 203–234

Hinz M, Stilmann M, Arslan Sc, Khanna KK, Dittmar G, Scheidereit C (2010) A cytoplasmic ATM-TRAF6-cIAP1 module links nuclear DNA damage signaling to ubiquitin-mediated NF-kappaB activation. *Mol Cell* **40:** 63–74

Huang TT, Wuerzberger-Davis SM, Wu ZH, Miyamoto S (2003) Sequential modification of NEMO/IKKgamma by SUMO-1 and ubiquitin mediates NF-kappaB activation by genotoxic stress. *Cell* **115:** 565–576

Iwai K (2012) Diverse ubiquitin signaling in NF-κB activation. *Trends Cell Biol* **22:** 355–364

Iwasaki H, Takeuchi O, Teraguchi S, Matsushita K, Uehata T, Kuniyoshi K, Satoh T, Saitoh T, Matsushita M, Standley DM, Akira S (2011) The I[kappa]B kinase complex regulates the stability of cytokine-encoding mRNA induced by TLR-IL-1R by controlling degradation of regnase-1. *Nat Immunol* **12:** 1167–1175

Jackson SP, Bartek J (2009) The DNA-damage response in human biology and disease. *Nature* **461:** 1071–1078

Janssens S, Tinel A, Lippens S, Tschopp J (2005) PIDD mediates NF-kappaB activation in response to DNA damage. *Cell* **123:** 1079–1092

Keusekotten K, Elliott Paul R, Glockner L, Fiil Berthe K, Damgaard Rune B, Kulathu Y, Wauer T, Hospenthal Manuela K, Gyrd-Hansen M, Krappmann D, Hofmann K, Komander D (2013) OTULIN antagonizes LUBAC signaling by specifically hydrolyzing Met1-linked polyubiquitin. *Cell* **153:** 1312–1326

Komander D, Reyes-Turcu F, Licchesi JDF, Odenwaelder P, Wilkinson KD, Barford D (2009) Molecular discrimination of structurally equivalent Lys 63-linked and linear polyubiquitin chains. *EMBO Rep* **10:** 466–473

Lee MH, Mabb AM, Gill GB, Yeh ET, Miyamoto S (2011) NF-[kappa]B induction of the SUMO protease SENP2: a negative feedback loop to attenuate cell survival response to genotoxic stress. *Mol Cell* **43:** 180–191

Liang J, Saad Y, Lei T, Wang J, Qi D, Yang Q, Kolattukudy PE, Fu M (2010) MCP-induced protein 1 deubiquitinates TRAF proteins and negatively regulates JNK and NF-kappaB signaling. *J Exp Med* **207:** 2959–2973

Liang J, Wang J, Azfer A, Song W, Tromp G, Kolattukudy PE, Fu M (2008) A novel CCCH-zinc finger protein family regulates proinflammatory activation of macrophages. *J Biol Chem* **283:** 6337–6346

Liu J, Xia H, Kim M, Xu L, Li Y, Zhang L, Cai Y, Norberg HV, Zhang T, Furuya T, Jin M, Zhu Z, Wang H, Yu J, Li Y, Hao Y, Choi A, Ke H, Ma D, Yuan J (2011) Beclin1 controls the levels of p53 by regulating the deubiquitination activity of USP10 and USP13. *Cell* **147:** 223–234

Mabb AM, Wuerzberger-Davis SM, Miyamoto S (2006) PIASy mediates NEMO sumoylation and NF-kappaB activation in response to genotoxic stress. *Nat Cell Biol* **8:** 986–993

Matsushita K, Takeuchi O, Standley DM, Kumagai Y, Kawagoe T, Miyake T, Satoh T, Kato H, Tsujimura T, Nakamura H, Akira S (2009) Zc3h12a is an RNase essential for controlling immune responses by regulating mRNA decay. *Nature* **458:** 1185–1190

McCool KW, Miyamoto S (2012) DNA damage-dependent NF-kappaB activation: NEMO turns nuclear signaling inside out. *Immunol Rev* **246:** 311–326

Niu J, Shi Y, Iwai K, Wu Z-H (2011) LUBAC regulates NF-[kappa]B activation upon genotoxic stress by promoting linear ubiquitination of NEMO. *EMBO J* **30:** 3741–3753

Niu J, Shi Y, Tan G, Yang CH, Fan M, Pfeffer LM, Wu ZH (2012) DNA damage induces NF-kappaB-dependent microRNA-21 up-regulation and promotes breast cancer cell invasion. *J Biol Chem* **287:** 21783–21795

Perkins ND (2007) Integrating cell-signalling pathways with NF-kappaB and IKK function. *Nat Rev Mol Cell Biol* **8:** 49–62

Rashi-Elkeles S, Elkon R, Weizman N, Linhart C, Amariglio N, Sternberg G, Rechavi G, Barzilai A, Shamir R, Shiloh Y (2006) Parallel induction of ATM-dependent pro- and antiapoptotic signals in response to ionizing radiation in murine lymphoid tissue. *Oncogene* **25:** 1584–1592

Rieser E, Cordier SM, Walczak H (2013) Linear ubiquitination: a newly discovered regulator of cell signalling. *Trends Biochem Sci* **38:** 94–102

Rivkin E, Almeida SM, Ceccarelli DF, Juang Y-C, MacLean TA, Srikumar T, Huang H, Dunham WH, Fukumura R, Xie G, Gondo Y, Raught B, Gingras A-C, Sicheri F, Cordes SP (2013) The linear ubiquitin-specific deubiquitinase gumby regulates angiogenesis. *Nature* **498:** 318–324

Ruland J (2011) Return to homeostasis: downregulation of NF-[kappa]B responses. *Nat Immunol* **12:** 709–714

Simonson SJ, Wu ZH, Miyamoto S (2007) CYLD: a DUB with many talents. *Dev Cell* **13:** 601–603

Skalniak L, Mizgalska D, Zarebski A, Wyrzykowska P, Koj A, Jura J (2009) Regulatory feedback loop between NF-κB and MCP-1-induced protein 1 RNase. *FEBS J* **276:** 5892–5905

Soncini C, Berdo I, Draetta G (2001) Ras-GAP SH3 domain binding protein (G3BP) is a modulator of USP10, a novel human ubiquitin specific protease. *Oncogene* **20:** 3869–3879

Stilmann M, Hinz M, Arslan SC, Zimmer A, Schreiber V, Scheidereit C (2009) A nuclear Poly(ADP-Ribose)-dependent signalosome confers DNA damage-induced IkB kinase activation. *Mol Cell* **36:** 365–378

Suzuki HI, Arase M, Matsuyama H, Choi YL, Ueno T, Mano H, Sugimoto K, Miyazono K (2011) MCPIP1 ribonuclease antagonizes dicer and terminates MicroRNA biogenesis through precursor microRNA degradation. *Mol Cell* **44:** 424–436

Tergaonkar V, Perkins ND (2007) p53 and NF-κB crosstalk: IKKα tips the balance. *Mol Cell* **26:** 158–159

Wu ZH, Shi Y, Tibbetts RS, Miyamoto S (2006) Molecular linkage between the kinase ATM and NF-kappaB signaling in response to genotoxic stimuli. *Science* **311:** 1141–1146

Wu ZH, Wong ET, Shi Y, Niu J, Chen Z, Miyamoto S, Tergaonkar V (2010) ATM- and NEMO-dependent ELKS ubiquitination co-ordinates TAK1-mediated IKK activation in response to genotoxic Stress. *Mol Cell* **40:** 75–86

Xu J, Peng W, Sun Y, Wang X, Xu Y, Li X, Gao G, Rao Z (2012) Structural study of MCPIP1 N-terminal conserved domain reveals a PIN-like RNase. *Nucleic Acids Res* **40:** 6957–6965

Xu M, Skaug B, Zeng W, Chen ZJ (2009) A ubiquitin replacement strategy in human cells reveals distinct mechanisms of IKK activation by TNFalpha and IL-1beta. *Mol Cell* **36:** 302–314

Yang Y, Xia F, Hermance N, Mabb A, Simonson S, Morrissey S, Gandhi P, Munson M, Miyamoto S, Kelliher MA (2011) A cytosolic ATM/NEMO/RIP1 complex recruits TAK1 to mediate the NF-{kappa}B and p38 MAP kinase/MAPKAP-2 responses to DNA damage. *Mol Cell Biol* **31:** 2774–2786

Yuan J, Luo K, Zhang L, Cheville JC, Lou Z (2010) USP10 regulates p53 localization and stability by deubiquitinating p53. *Cell* **140:** 384–396

Zhang L, Ding X, Cui J, Xu H, Chen J, Gong Y-N, Hu L, Zhou Y, Ge J, Lu Q, Liu L, Chen S, Shao F (2012) Cysteine methylation disrupts ubiquitin-chain sensing in NF-[kgr]B activation. *Nature* **481:** 204–208

Zhou L, Azfer A, Niu J, Graham S, Choudhury M, Adamski FM, Younce C, Binkley PF, Kolattukudy PE (2006) Monocyte chemoattractant protein-1 induces a novel transcription factor that causes cardiac myocyte apoptosis and ventricular dysfunction. *Circ Res* **98:** 1177–1185